ISSN: 2278-4632
Vol-13, Issue-01, No.03, January 2023

IMPLEMENTATION OF MULTIFUNCTIONAL ELECTRICVEHICLE CHARGER BASED ON ANFIS WITH SOLAR PV ARRAY

Dr. S.Hussain Vali[1], Othuru Baba [2], V.Rafi[3]
[1-3] Department of Electrical and Electronics Engineering, JNTUA College of Engineering Pulivendula, Kadapa, India.
Corr.author mail: vempallerafi@gmail.com

Abstract: - This paper describes the development of a grid-connected, domestic electric vehicles (EV) charger that is powered by solar photovoltaic (PV) arrays and meets the need of an EV, household loads, and the grid. With the help of PV array, the charger is equipped to run independently while supplying uninterrupted power and charging to home loads. However, the grid linked mode of operation is offered if there is no PV array or inadequate PV array generation. The charger is supported by synchronization and smooth mode switching management, enabling automated grid connection and disconnection without interfering with the EV charging or household supply. The charger is additionally equipped with active/reactive power support from the vehicle to the grid (V2G) and power transfer from the vehicle to the home (V2H) for sustaining the local loads in an isolated situation. Additionally, the charger is regulated to function as an active power filter to maintain the grid current's total harmonic distortion (THD) within 5% and run at unity power factor (UPF). A dc-link voltage regulation based energy management technique is employed to achieve energy management, and an adaptive neuro-fuzzy inference system (ANFIS) is used to regulate the dc-link voltage.

Keywords: - Adaptive Neuro-fuzzy Inference System *(*ANFIS), Electric vehicle, Solar PV generation, Power quality, Active power and Reactive power.

INTRODUCTION

The electric vehicle (EV) is gaining popularity as a viable alternative to nonrenewable fuel-powered automobiles at the moment [1]. The infrastructure for charging EVs, however, is crucial [2]. Electricity used to charge EVs is extremely energy-intensive and is often produced by coal- and gas-fired power stations. Therefore, EVs may actually be a green and clean alternative to the current transportation system if the electrical energy needed to charge them comes from sources of renewable energy like solar, wind, and other similar sources. The fact that this type of charging station uses locally generated and consumed PV array power is a benefit. As a result, there is no need to improve the transmission lines to handle the high power. The charging station does not need to use the grid when energy prices are high. The installation of solar PV panels on office buildings and parking lots has been suggested.

In this paper, the solar PV array is directly linked to the dc connection in this article. The deletion of the dc-dc converter step reduces the number of power stages by one, reduces circuit complexity, and lowers converter cost without reducing the PV array's performance.

In order to increase the charger's operating efficiency while the EV is not connected for charging, the converter must be used for other purposes. Numerous capabilities have been suggested in the literature, including active filtering, vehicle-to-home operation utilizing an EV battery, and four-quadrant charger operation. However, the literature that is now accessible uses a number of converters and controllers for a variety of working modes. Additionally, the charger's capacity to operate is constrained by the grid's accessibility (islanded or grid linked operation), the manner in which modes are switched between them (seamless or discontinuous), and other factors that have an impact on the charger's operational effectiveness. However, the review shows that the majority of the recent literature is theoretical research, and very few publications have actually used the solar PV array- based EV charger, which is capable of carrying out the aforementioned functionalities using a mono topological features and unified control.

The integration of EV charging with a renewable source, residential load, and the grid, however, poses problems for the system's overall energy management. A unique predictive fuzzy logic-based energy management system for a grid-integrated micro grid has been suggested. The controller makes use of the system's long-term data to forecast energy output, demand, and cost. The development of a rule- and optimization-based energy management system has been the focus of several studies. The heuristic rule governs how the microgrid operates in the regulation method. The heuristic-based rule's disadvantage is that it is microgrid -specific. As a result, designing generic rules is not possible. The day-ahead prediction is used by the energy management system with centralized optimization to optimize the functioning of the microgrid. The day ahead scheduling, however, cannot deliver adequate performance because to the significant unpredictability and uncertainty in the renewable generation, load, and poor forecast accuracy. However, the promptness and accuracy of the dc-link voltage controller determine how well the energy management plan works. In order to construct the increased dc voltage control loop, the method for cancelling the second harmonic ripple in the dc-link voltage. The robust dc bus voltage control loop for efficient power-sharing. In a three-phase power converter, unified control maintains the dc-link voltage using a ANFIS controller. Similar to this, a PI controller is used in many other publications to control the dc bus voltage. Because of this, it is impossible to tune the ANFIS controller to accommodate the unknown disturbances while it is operating. In order to enhance the system's dynamic and steady-state performances, the dc-link voltage control in this research uses an adaptive neuro-fuzzy inference system (ANFIS). The

ANFIS is well renowned for its remarkable resilience to disturbances and uncertainties, such as unidentified fluctuations in control variables and system parameters.

The benefit of this system is that it can handle utility, EV, and home load requirements with only one system. These are the primary characteristics of this system.

- Using a PV array in both an islanded and a grid-connected mode to power domestic loads and charge EVsconcurrently.
- Creation of a reliable control technique for producing a sinusoidal voltage at the PCC with a totalharmonic distortion (THD) of around 4%.
- Using vehicle-to-home (V2H) capabilities, EV batteries may be used to power the household loadcontinuously while operating in an island environment.
- Creation of a control system to synchronize grid and PCC voltage as well as logic to provide switch enablinglogic (E) for a smooth move from islanded to grid connected mode.
- Active power filter operation using VSC, preventing grid pollution from the charger.
- The ability to provide reactive electricity from a vehicle to the grid (V2G) on demand utilizing the EV batteryand VSC.

I. SYSTEM CONFIGURATION

The circuit topology of the presented charging system isshown in Fig. 1. This device combines a solar PV array right into the VSC's de-link, making it a single-phase, bi-directional EV charger. This system sends solar PV and EV battery electricity into the grid while simultaneously charging the EV battery with grid and solar PV power. A bi-directional ac-de conversion stage is followed by a bi-directional de-de conversion stage in this charger's two-stage design. The ac-dc conversion stage serves as an inverter to transform the de voltage into the ac voltage when supplying solar PV power and EV electricity to the grid. It also changes the input ac voltage into the de voltage while charging the EV battery. The EV battery is connected to the output of the bidirectional de-de converter (BDDC). The dc-dc converter in the charger performs all required tasks. The dc converter operates in boost mode while the EV battery is being discharged and in buck mode when theEV battery is being recharged.

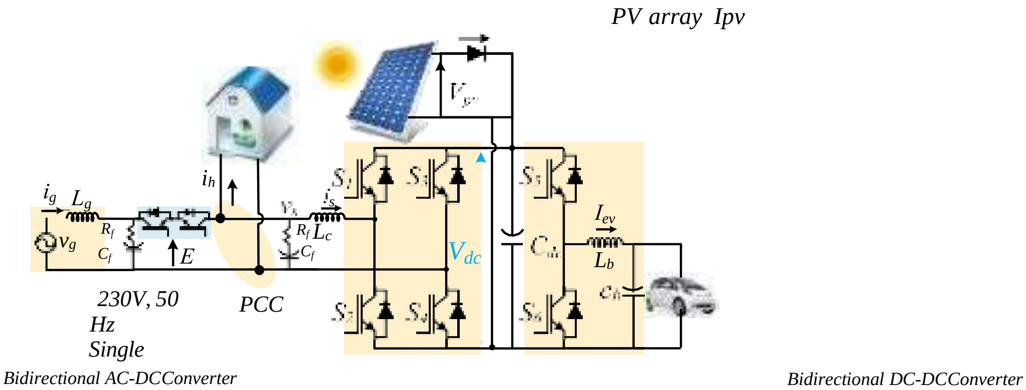

Fig: - 1 Circuit topology of charger.

Additionally, it controls the dc bus voltage and maximizes the power provided by the solar PV array. The coupling inductor connects the charger to the grid (Lc). Harmonics must be removed in order to smooth the grid current. To stop switching harmonics produced by the VSC from being injected into the grid, a ripple filter is additionally attached at the PCC (Point of Common Coupling).

ISSN: 2278-4632
Vol-13, Issue-01, No.03, January 2023

II. ENERGY MANAGEMENT STRATEGY

This charger's energy management method is based on the control of a constant dc-link voltage. Fig. 2 displays the flowchart of energy management under various operating situations. The steady-state energy management in grid-connected mode is provided as,

$$P_{PV} \pm P_B \pm P_g - P_h = 0 \qquad (1)$$

Here, PPV, PEV, Ph, and Pg. represent the power from a solar PV array, an EV, a residential load, and the grid, respectively. The positive power in this statement denotes the generation of power, while the negative power denotes its consumption. This implies that both the grid and the EV may produce and consume energy. The charger experiences a transient in grid linked mode as a result of changes inisolar irradiance, home load, and EV charging current. The charging/discharging of the EV battery and household supply shouldn't be impacted by the change in PV array power because it solely affects the grid power.

As a result, a number of things happen in order to reach the systems energy equilibrium during an irradiance shift.

Solar irradiance $\uparrow\downarrow \rightarrow P_{PV}\uparrow\downarrow \rightarrow$ power at dc-link $\uparrow\downarrow$

$$\rightarrow V_{dc}\uparrow\downarrow \rightarrow V_{dc} \text{ regulation} \rightarrow I_P\uparrow\downarrow \rightarrow i^*_g\uparrow\downarrow \rightarrow i_g\uparrow\downarrow \qquad (2)$$

In standalone mode, the steady-state energy management is provided as,

$$P_{PV} \pm P_{EV} - P_h = 0 \qquad (3)$$

The change in home demand and solar irradiation both affect the energy balance in standalone mode,just like they do in grid-connected mode. However, because the dc-link voltage is regulated by the EV battery, it adjusts for any power interruptions. Energy management is achieved under household load changes is given as,

$i_h\uparrow\downarrow \rightarrow$ power at dc-link $P_{PV}\uparrow\downarrow \rightarrow V_{dc}\uparrow\downarrow$

$$\rightarrow V_{dc} \text{ regulation} \rightarrow I_{EV}\uparrow\downarrow \rightarrow I_{EV}\uparrow\downarrow \qquad (4)$$

III. CONTROL ALGORITHM

The control goal is to continuously power the home without interruption while charging the electric vehicle. As a result, the control is created in a way that allows for multipurpose operation. The control is essentially divided into islanded and grid linked modes, as shown in Fig. 3. (GCM). The active and reactive powers as well as the vehicle-to-home (V2H) modes of the vehicle-to-grid (V2G) are, however, covered by these two main controllers. Additionally, both islanded and grid connected approaches of combined bi-directional control of dc-dc converters are investigated.

A. *Grid Connected Mode Control*

In order to control the active and reactive power flow and produce switching pulses for the VSC, the GCM mode regulates the dc link voltage and grid current. Here is an explanation of ANFIS and variable speed control.

1) *ANFIS of dc Link Voltage*

In this project, ANFIS is used to control the solar PV array's maximum power point tracking (MPPT) and dc-link voltage. As in single-stage topology, the MPPT is accomplished by regulating the dc-link at the solar PV array's MPP voltage, the dc-link voltage control is also necessary for the MPPT of the solar PV array.

The surface of the sliding mode control is created using a mix of proportional and integral functions of voltage error because the ANFIS regulates the de-link voltage. To regulate the reaching and sliding dynamics of the controller, the proportional and integral kind of sliding surface is used. When the voltage error is high at first, the proportional term moves the error close to the surface, and once there, the integral term regulates the voltage error's sliding at the surface. The voltage error is expressed as,

$$e = V^*_{dc} - V_{dc} \qquad (5)$$

The net instantaneous active power flow determines how much voltage the dc-link will have. The de-link voltage rises when the net instantaneous active power flow turns positive. However, with net negative instantaneous active power flow, the de-link voltage falls. As a result, fast calculation of the loss component of the reference grid current and de-link voltage regulation are required for regulating the active power balance in the system. This work uses a sliding surface to pick the voltage error as the surface, which is dependent on the net active power flow. Using the sliding surface, the estimated current is expressed as,

$$I_{dc} = \begin{cases} P^+_{dc}, & S>0 \\ P^-_{dc}, & S<0 \end{cases} \qquad (6)$$

The first-order derivative of the dc-link voltage isnow derived as follows.

 ISSN: 2278-4632
Vol-13, Issue-01, No.03, January 2023

$$\dot{V}_{dc} = \frac{I_d}{C_{dc}V_{dc}} - \frac{1}{R_L C_{dc}} V_{dc} + \mu \tag{7}$$

Based on the Lyapunov stability requirements, which specify that, the controller for dc-link voltagemanagement and for calculating the loss component of current is created.

$$S\{\gamma\,(\dot{V}_{dc} - \dot{V}_{dc}^{*}) + e\} = S\{\gamma\,(\dot{V}_{dc}) + e\} \tag{8}$$

$$S\{\gamma(\frac{I_d}{C_{dc}V_{dc}} - \frac{1}{R_L C_{dc}} V_{dc} + \mu) + e\} \tag{9}$$

$$S\{(\frac{\gamma I_d}{C_{dc}V_{dc}} - \frac{\gamma}{R_L C_{dc}} V_{dc} + \gamma\mu) + e\} \tag{10}$$

Now, Id is selected such that $S.S < 0$

$$I_d = C_{dc}V_{dc}\left[\left(\frac{1}{R_L C_{dc}} - \frac{1}{\gamma}\right)V_{dc} + \frac{1}{\gamma}V_{dc}^{*} - (\sigma + \delta)\text{sign}(S)\right] \tag{11}$$

The chattering phenomena may emerge with the current ANFIS control because of the (σ + δ) sign(S). With the current ANFIS control, the chattering cannot be completely eradicated. But by determining the lowest permitted steady-state error and setting the value of so that the (+) does not get too tiny, the chattering has been kept to a specific frequency. Since is a positive constant, the definition of is as follows:

$$\delta = \begin{cases} \| e \| & , v_e > 0.1V \\ .1 & v_e < 0.1V \end{cases} \tag{12}$$

2) *VSC Control in GCM*

VSC control is shown in Fig. 3. The EV and non-linear domestic loads are to blame for the harmonics in the grid current. Moreover, the power factor (PF) also deteriorates. Therefore, a second-order generalized integrator-frequency locked loop with dc rejection capacity (SOGI-FLL-DR) is utilized to estimate the fundamental load current so that the reference current becomes harmonic-free in order to improve the PF and guarantee the grid current THD under 4%. Using sample hold and ZCD, Fig. 3 illustrates the extraction of the basic active load current component (Zero Crossing Detector). The active current estimate expression is provided as

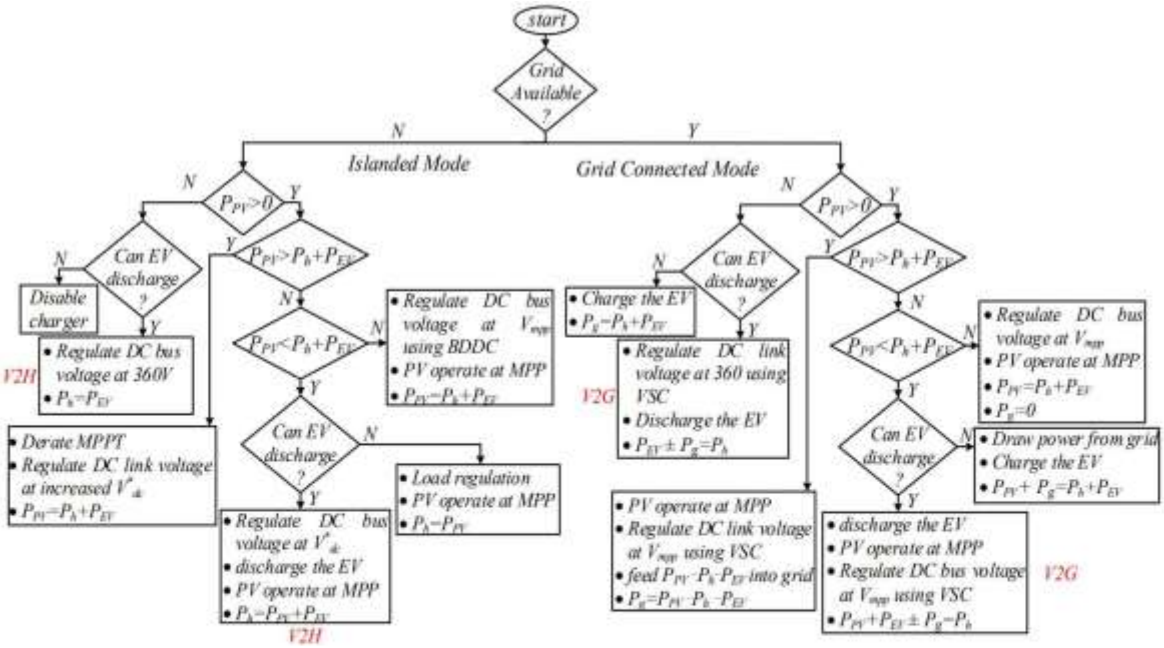

Fig: - 2 Flowchart of energy management and operation strategy.

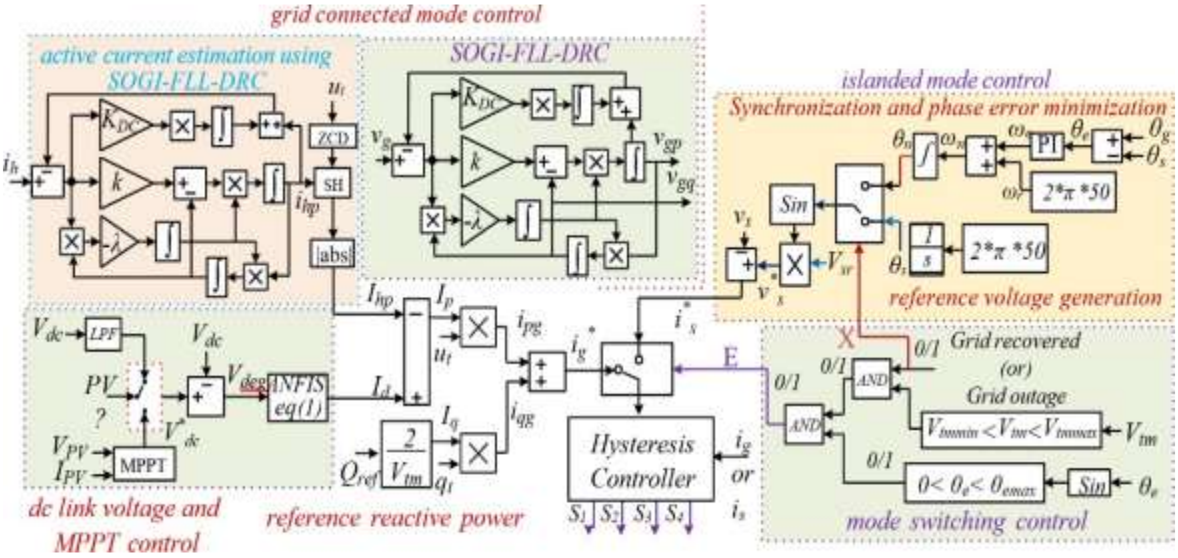

Fig: - 3 Combined control strategy for VSC

$$\frac{i_{hp}}{i_h} = \frac{k\omega s^2}{s^3 + (k_o + k\omega)s^2 + \omega^2(s + k_o)} \tag{13}$$

Where the load currents ih and ihp are the basic load currents. is the frequency prediction coefficient, ko is the dc rejection coefficient, k is a gain that controls the speed of prediction, and is the frequency.The calculated total active current is as follows using (11) and Ihp:

$$I_p = I_d - I_{hp} \tag{14}$$

The reference grid current's reactive current's amplitude (Iq) is calculated using the referencereactive power command (Qref), and it is stated as,

$$I_q = \frac{2 \times Q_{ref}}{V_{tm}} \tag{15}$$

Where V_{tm} is the amplitude of the PCC voltage (v_s).

Instantaneous reference active grid current (ip) and instantaneous reference reactive grid current (iq) are obtained by multiplying the real (Ip) and reactive (Iq) components by the in-phase (ut) and quadrature-phase unit template (qt), and they are provided as,

$$i_p = I_p \times u_t,\ i_q = I_q \times q_t \tag{16}$$

Using the following formulas, the in-phase (ut) and quadrature-phase unit template (qt) are produced.

$$u_t = \frac{v_{gp}}{V_{tm}},\ q_t = \frac{v_{gq}}{V_{tm}} \tag{17}$$

Where Vtm is the PCC voltage's amplitude and Vgp and Vgq are its in-phase and quadrature-phase voltages, respectively. The predicted unit templates also become sinusoidal since these two voltages (Vg and Vs) computed using the SOGI-FLL-DR method become harmonic-free.With the aid of Vpg and Vgq, the Vtm is produced as,

$$V_{tm} = \sqrt{v_{gp}^2 + v_{gq}^2} \tag{18}$$

The total reference grid current is calculated using the reference active grid current (ip) and reference reactive grid current (iq).

$$i_g^* = i_p + i_q \tag{19}$$

The hysteresis controller creates the triggering signals for the VSC by comparing the detected grid current (ig) with this reference grid current (ig*).

B. VSC Control in Islanded Mode

The integrated system's goal in islanded mode is to use the PV array energy to autonomously power the household load and charge the EV. In addition, the V2H power transfer is used to provide the home load when the PV array is not producing any electricity. When the VSC is in the islanded mode, it is regulated to function as an inverter to provide the load in accordance with the control illustrated iniFig.3. To do this, the controller produces the voltage as seen in Fig. 3iutilizing the reference frequency and voltage.

The reference voltage and the observed voltage are used to create the VSC pulses. The charger requires a grid connection to operate in "islanded mode" and exchange two-way electricity. As a result, the grid voltage, frequency, and phase must match the PCC voltage, frequency, and phase. Such that the grid connection is automatic and smooth. In order to determine the phase error between two voltages, the controller estimates the phase angles of the grid voltage and PCC voltage. The phase error between two volts is reduced using the PI controller. The PI controller transforms the phase error data into error frequency. Using the erroneous frequency, the controller generates the reference voltage for the corrected frequency. As soon as the phases of two voltages are in phase with one another, the controller generates the enabling signal for the bidirectional switch inline with the switching logic shown in Fig. 3.

IV. RESULTS AND DISCUSSION

The open-circuit voltage and short circuit current of the solar PV array are 460V and 10A, respectively. However, the greatest power point voltage and current are 396 V and 9.5 A, respectively. The EV battery in the experimental model is a 240V, 35Ah lead-acid battery. The digital controller is used to operate the charger (dSPACE-1006). Various signals (voltage and current) from the charger are required by the digital controller in order to carry out the control algorithm. A range of voltage and current signals may be obtained using the Hall Effect-based voltage (LEM LV-25P) and current (LEMiLA-55P) sensors (analogue). These signals are converted from analogue to digital using an analogue to digital converter (ADC). The digital controller processes the digital signal, applies the control algorithm, and generates the switching pulses for the VSC and dc-dc converter.

A. Steady-State Performance of Charger

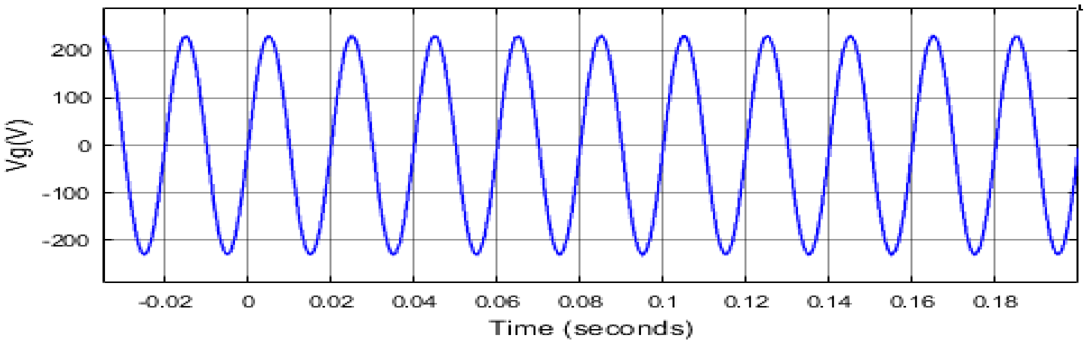

Fig: - 4(a) Grid voltage (V)

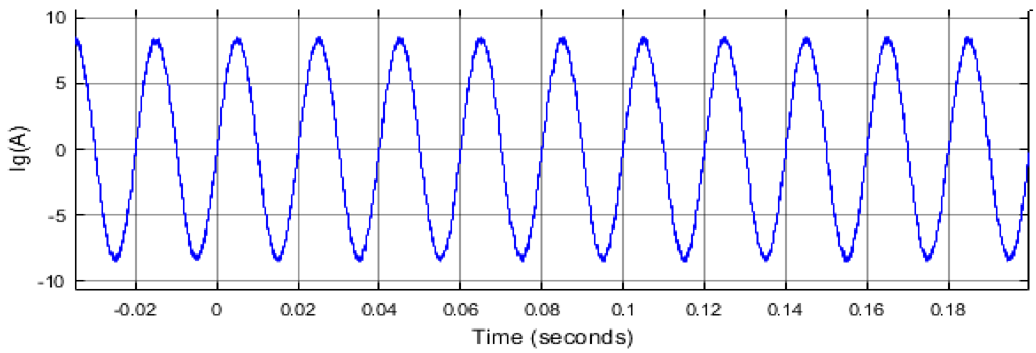

Fig: - 4(b) Grid Current (A)

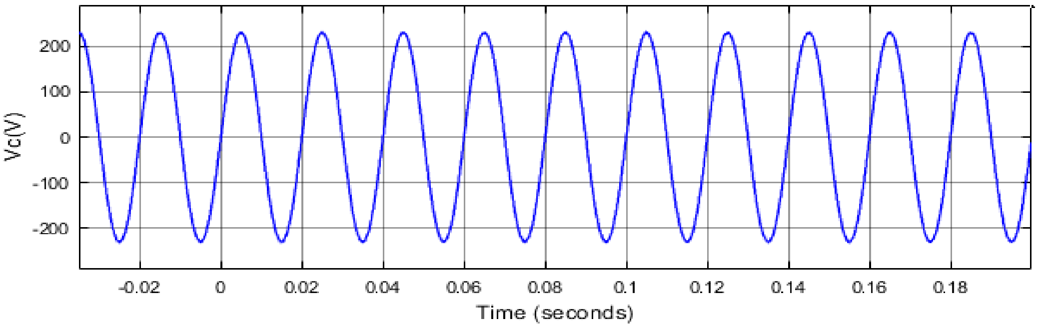

Fig: - 4(c) Charging Voltage (V)

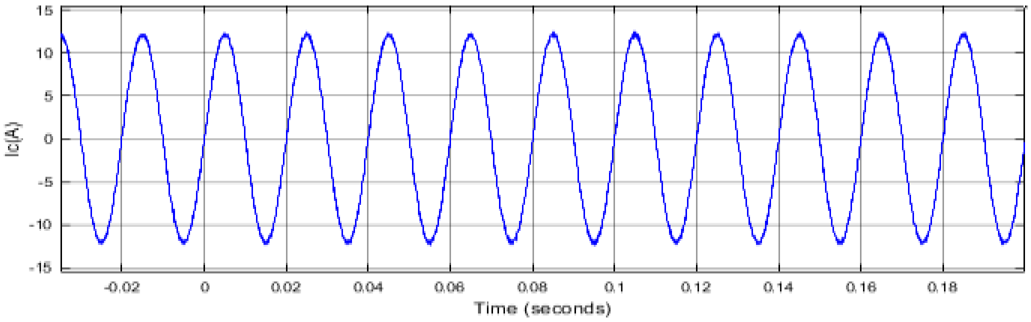

Fig: - 4(d) Charging Current (A)

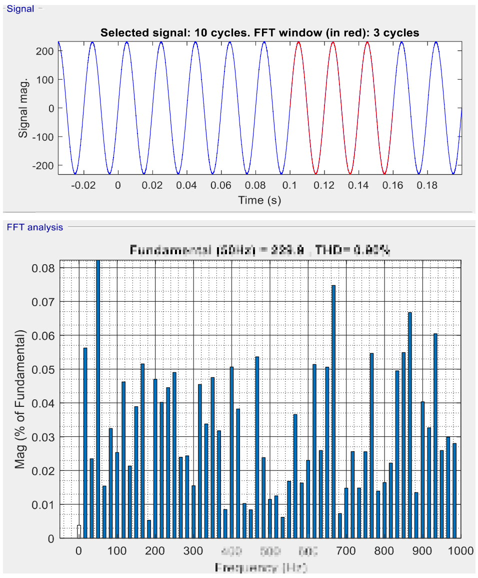

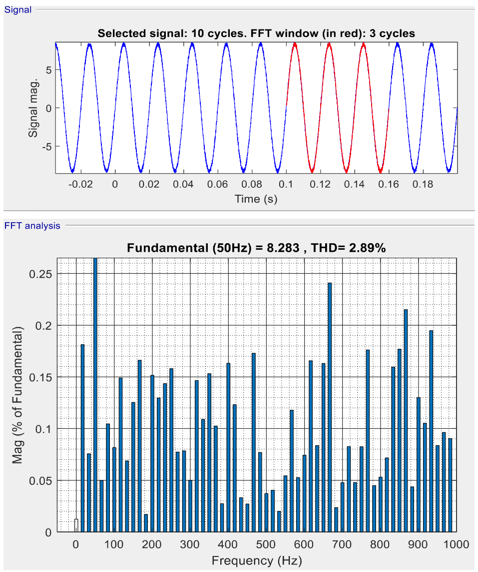

Fig: - 4(e) THD of Vgv Fig: - 4(f) THD of Igv

The charger is not adding any voltage or current harmonics to the grid, based on the grid voltage (vg), grid current (ig), and load current. (ih), Total harmonic distortion (THD) is seen in Figs (i). The charger in Fig. is operating at unity displacement power factor (DPF), indicating that it is not utilizing any reactive power from the grid. In Fig. the VSC parameters are shown.

B. Dynamic Performance of Charger

The charger's independence in running an EV charging station and providing electricity to a home's load using power from a solar PV array is highlighted by a demonstration of the charger in its isolated mode. When the solar irradiation is operating in the islanded mode, the residential load varies. As a consequence, Fig. 7 illustrates how the charger functions when there are disruptions.

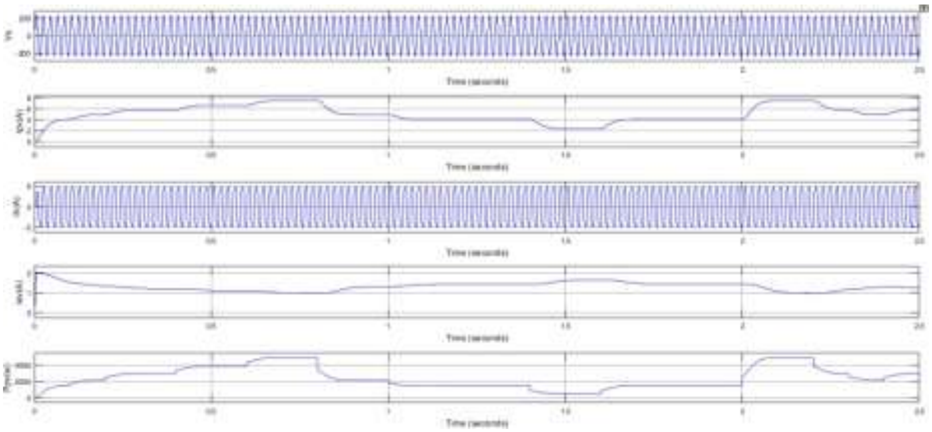

Fig: - 5(a) under change in household load

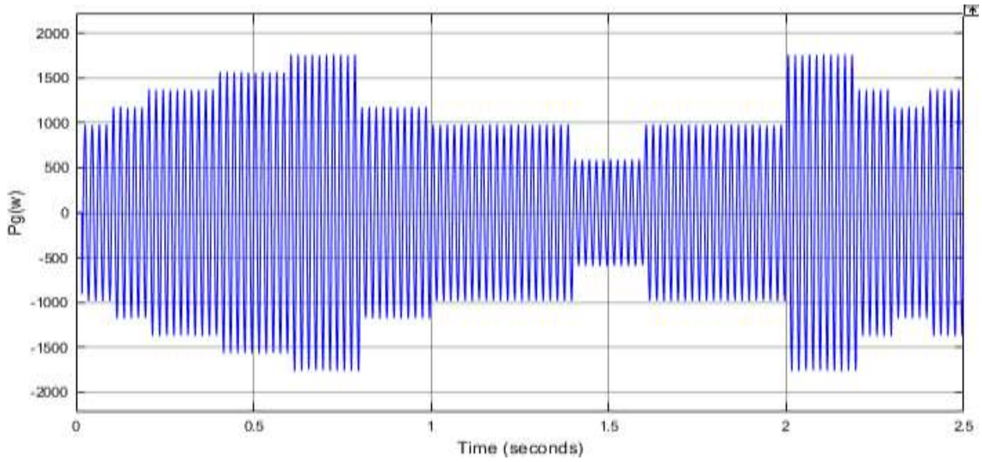

Fig: - 5(b) Generator power

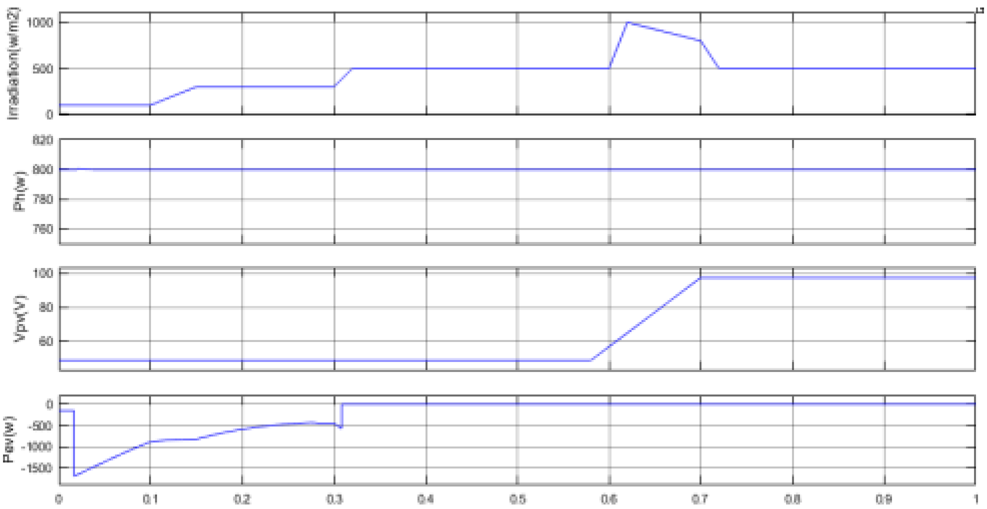

Fig: - 5(c) derating of MPPT

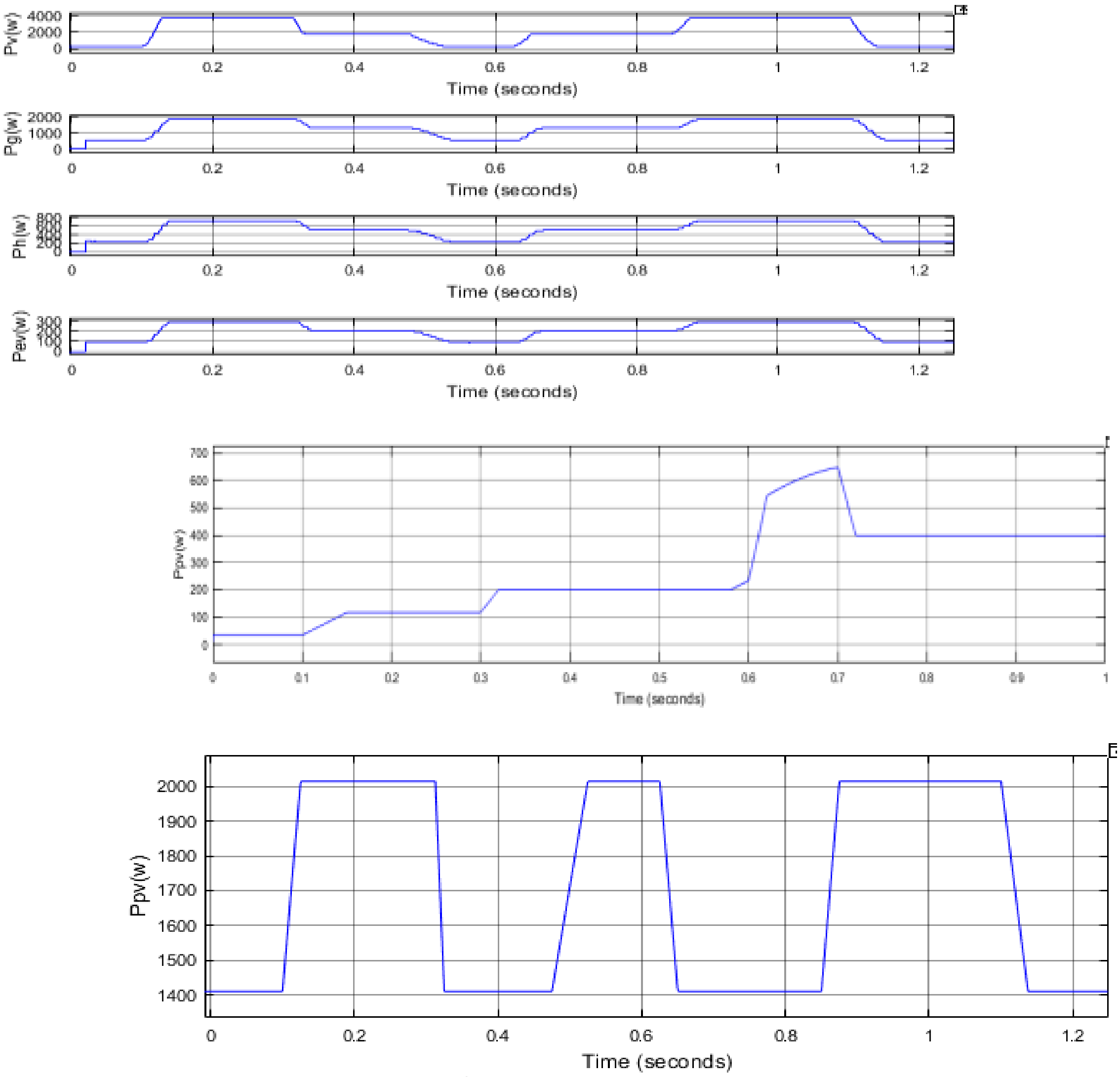

Fig: - 5(d) Performance under change in solar irradiance power

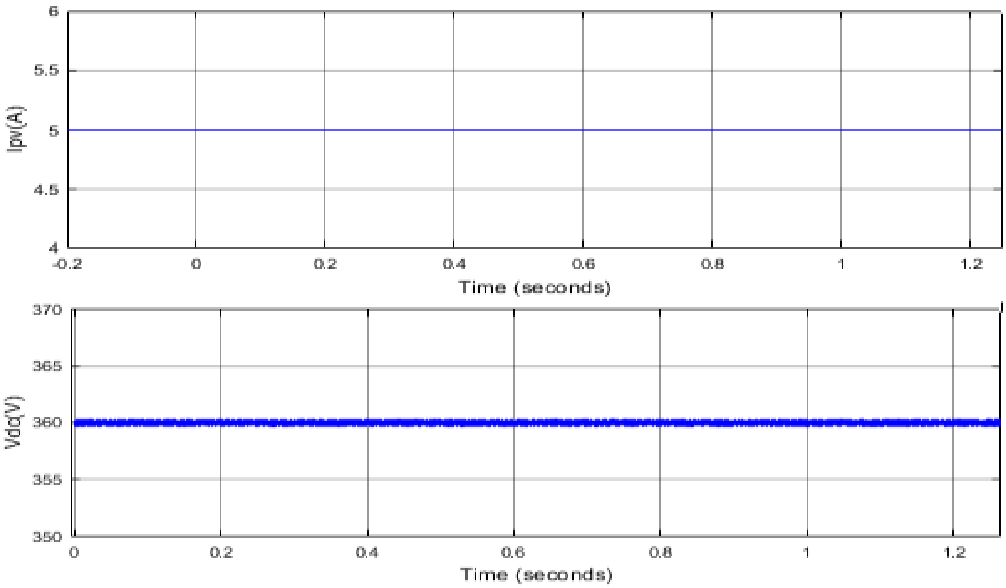

Fig: - 5(e) Voltage and current under charging and discharging of EV battery

ISSN: 2278-4632
Vol-13, Issue-01, No.01,January 2023

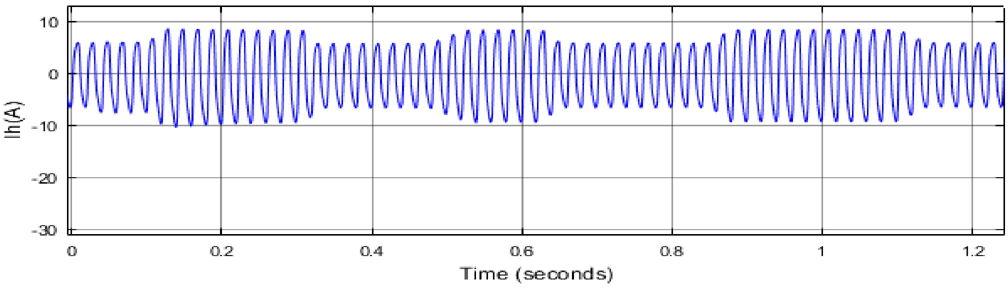

Fig: - 5(f) Household current

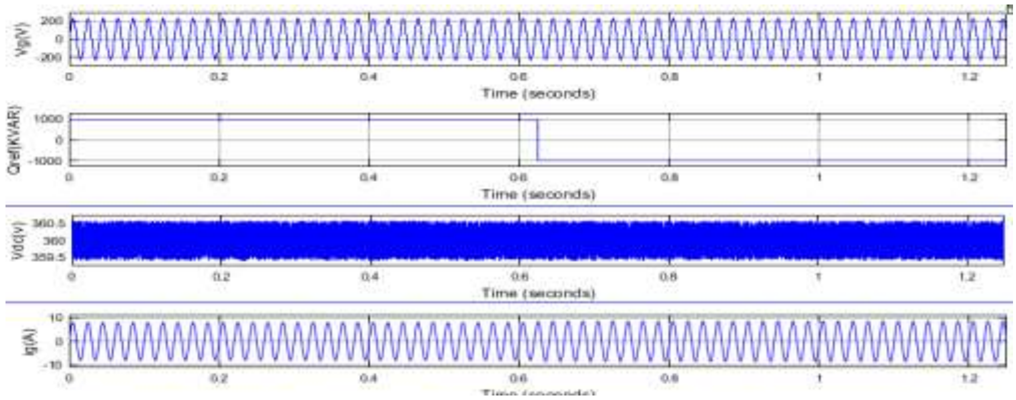

Fig: - 6 Reactive power performance of vehicle to grid

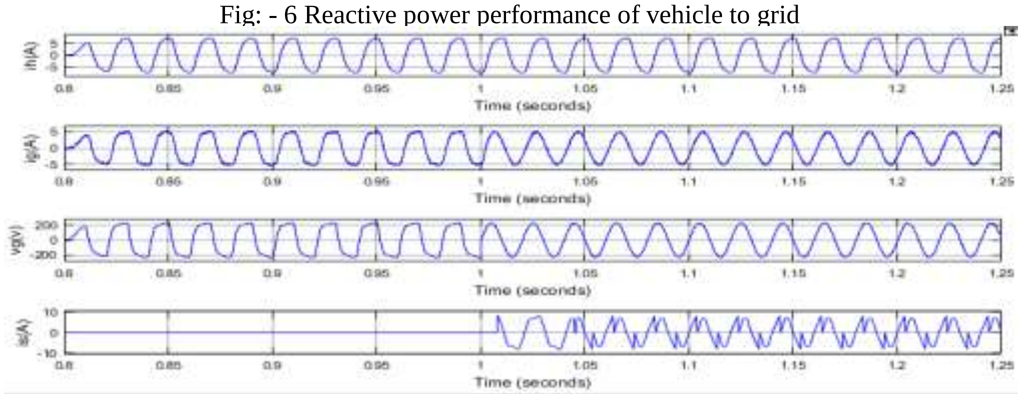

Fig: - 7 Active power filter and distorted voltage condition operation performance

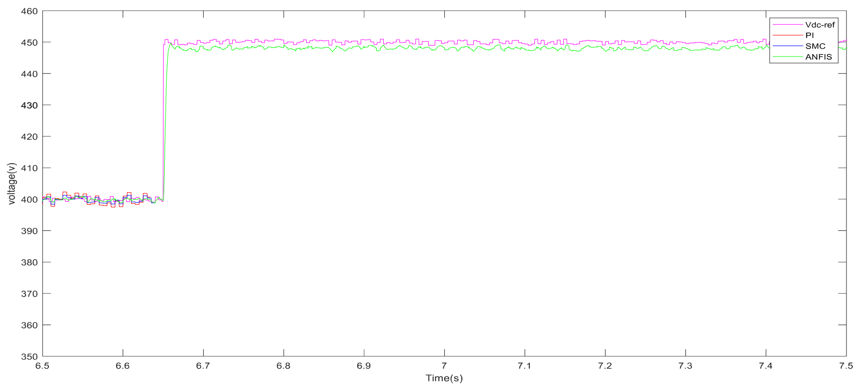

Fig: - 8 Comparison of dc-link voltage regulation using PI, SMC and ANFIS

The capacity of the PI controller, SMC, and ANFIS to regulate the dc-link voltage (Vdc) under a step change of 50Vkin the reference dc-link voltage (V*) is shown in Fig. 8. As seen in Fig. 8, the ANFIS regulates the dc-link voltage more quickly than the PI control and SMC.

V. CONCLUSION

An integrated charger with solar PV array, household load and grid has been implemented. The test result have confirmed that the simultaneous EV charging and household supply in both islanded and grid connected modes. According to these test that the charger is doing what is supposed to be doing charging EVs. Serving loads and maintaining grid power quality.

REFERENCES

[1] Anjeet Verma, Bhim Singh, Ambrish Chandra, Kamal Al Haddad. "An Implementation of Solar PV Array Based Multifunctional EV Charger" , IEEE Transactions on Industry Applications, 2020

[2] J. R. Aguero, E. Takayesu, D. Novosel and R. Masiello, "Modernizing the Grid: Challenges and Opportunities for a Sustainable Future," *IEEEPower and Energy Magazine*, vol. 15, no. 3, pp. 74-83, May-June 2017.

[3] D. Bowermaster, M. Alexander and M. Duvall, "The Need for Charging: Evaluating utility infrastructures for electric vehicles while providing customer support," *IEEE Electrifi. Mag.*, vol. 5, no. 1, pp. 59-67, 2017

[4] X. Lu and J. Wang, "A Game Changer: Electrifying Remote Communities by Using Isolated Microgrids," *IEEE Electrifi. Mag.*, vol. 5, no. 2, pp. 56- 63, June 2017.

[5] T. Ma and O. A. Mohammed, "Optimal Charging of Plug-in Electric Vehicles for a Car-Park Infrastructure," *IEEE Trans. Ind. Applicat.*, vol. 50, no. 4, pp. 2323-2330, July-Aug. 2014.

[6] L. Cheng, Y. Chang and R. Huang, "Mitigating Voltage Problem in Distribution System With Distributed Solar Generation Using Electric Vehicles," *IEEE Trans. Sust. Ene*, vol. 6, no. 4, pp. 1475-1484, Oct. 2015.

[7] S. J. Gunter, K. K. Afridi and D. J. Perreault, "Optimal Design of Grid- Connected PEV Charging Systems With Integrated Distributed Resources," *IEEE Trans. Smart Grid*, vol. 4, no. 2, pp. 956-967, 2013.

[8] A. S. Satpathy, N. K. Kishore, D. Kastha and N. C. Sahoo, "Control Scheme for a Stand-Alone Wind Energy Conversion System," *IEEE Trans. Energy Conversion*, vol. 29, no. 2, pp. 418-425, June 2014

[9] F. Marra, G. Y. Yang, C. Træholt and E. Larsen, "EV Charging Facilities and Their Application in LV Feeders With Photovoltaics," IEEE Trans. Smart Grid, vol. 4, no. 3, pp. 1533-1540, Sept. 2013.

[10] N. Saxena, I. Hussain, B. Singh and A. L. Vyas, "Implementation of a Grid-Integrated PV-Battery System for Residential and Electrical Vehicle Applications," IEEE Trans. Ind. Electron., vol. 65, no. 8, pp. 6592- 6601, Aug. 2018.

[11] V. Monteiro, J. G. Pinto and J. L. Afonso, "Experimental Validation of a Three-Port Integrated Topology to Interface Electric Vehicles and Renewables With the Electrical Grid," IEEE Trans. Industrial Informatics, vol. 14, no. 6, pp. 2364-2374, June 2018.

[12] V. T. Tran, K. M. Muttaqi and D. Sutanto, "A Robust Power Management Strategy With Multi-Mode Control Features for an Integrated PV and Energy Storage System to Take the Advantage of ToU Electricity Pricing," IEEE Trans. Ind. App., vol. 55, no. 2, pp. 2110-2120, 2019.

[13] A. Tazay and Z. Miao, "Control of a Three-Phase Hybrid Converter for a PV Charging Station," IEEE Trans. Energy Conver., vol. 33, no. 3, pp. 1002-1014, Sept. 2018.

[14] A. Verma, B. Singh, A. Chandra and K. Al-Haddad, "An Implementation of Solar PV Array Based Multifunctional EV Charger," in IEEE Transpo.. Electrifi. Conf. and Expo (ITEC), Long Beach, CA, 2018,pp. 531-536.

[15] A. Verma and B. Singh, "Multi-Objective Reconfigurable Three-Phase Off-Board Charger for EV," IEEE Trans. Ind. App., vol. 55, no. 4, pp. 4192-4203, July-Aug. 2019.

[16] H. Kikusato, K. Mori, S. Yoshizawa, Y. Fujimoto, H. Hiroshi, Y. Hayashi, A. Kawashima, S. Inagaki, T. Suzuki, "Electric Vehicle Charge– Discharge Management for Utilization of Photovoltaic by Coordination Between Home and Grid Energy Management Systems," IEEE Trans. Smart Grid, vol. 10, no. 3, pp. 3186-3197, May 2019.

[17] Y. Sun, H. Yue, J. Zhang and C. Booth, "Minimisation of Residential Energy Cost Considering Energy Storage System and EV with Driving Usage Probabilities," IEEE Trans. Sustainable Energy, Early Acsess.

[18] L. Bhamidi and S. Sivasubramani, "Optimal Planning and Operational Strategy of a Residential Microgrid With Demand Side Management," IEEE Systems Journal, Early Access.

[19] Y. Yang, Q. Jia, G. Deconinck, X. Guan, Z. Qiu and Z. Hu, "Distributed Coordination of EV Charging With Renewable Energy in a Microgrid of Buildings," IEEE Trans. Smart Grid, vol. 9, no. 6, pp. 6253-6264, 2018.

[20] K. Chaudhari, A. Ukil, K. N. Kumar, U. Manandhar and S. K. Kollimalla, "Hybrid Optimization for Economic Deployment of ESS in PV-Integrated EV Charging Stations," IEEE Trans. Ind. Informat., vol. 14, no. 1, pp. 106-116, Jan. 2018.

[21] A. Ravichandran, S. Sirouspour, P. Malysz and A. Emadi, "A ChanceConstraints-Based Control Strategy for Microgrids With Energy Storage and Integrated Electric Vehicles," IEEE Trans. Smart Grid, vol. 9, no.1, pp. 346-359, Jan. 2018.

[22] H. Turker and S. Bacha, "Optimal Minimization of Plug-In Electric Vehicle Charging Cost With Vehicle- to-Home and Vehicle-to-Grid Concepts," IEEE Trans. Veh. Tech.., vol. 67, no. 11, pp. 10281-10292, Nov.2018.

[23] O. Erdinc, N. G. Paterakis, T. D. P. Mendes, A. G. Bakirtzis and J. P. S. Catalão, "Smart Household Operation Considering Bi-Directional EV and ESS Utilization by Real-Time Pricing-Based DR," IEEE Trans. Smart Grid, vol. 6, no. 3, pp. 1281-1291, May 2015.

[24] H. R. Baghaee, M. Mirsalim, G. B. Gharehpetian and H. A. Talebi, "A Decentralized Power Management and Sliding Mode Control Strategy for Hybrid AC/DC Microgrids including Renewable Energy Resources," IEEE Trans. Ind. Informatics. Early Access.

[25] Z. Yi, W. Dong and A. H. Etemadi, "A Unified Control and Power Management Scheme for PV-Battery- Based Hybrid Microgrids for Both Grid-Connected and Islanded Modes," IEEE Trans. Smart Grid, vol. 9, no. 6, pp. 5975-5985, Nov. 2018.

[26] M. Kwon and S. Choi, "Control Scheme for Autonomous and Smooth Mode Switching of Bidirectional DC–DC Converters in a DC Microgrid," IEEE Trans. Power Electronics, vol. 33, no. 8, pp. 7094-7104, Aug. 2018.

[27] M. Jafari, Z. Malekjamshidi, J. Zhu and M. Khooban, "Novel Predictive Fuzzy Logic-Based Energy Management System for Grid-connected and Off-grid Operation of Residential Smart Micro-grids," IEEE Journal of Emerging and Selected Topics in Power Electronics, Early Access.

[28] S. A. Singh, G. Carli, N. A. Azeez and S. S. Williamson, "Modeling, Design, Control, and Implementation of a Modified Z-Source Integrated PV/Grid/EV DC Charger/Inverter," IEEE Trans. Industrial Electronics, vol. 65, no. 6, pp. 5213-5220, June 2018.

[29] M. Restrepo, J. Morris, M. Kazerani and C. A. Cañizares, "Modeling and Testing of a Bidirectional Smart Charger for Distribution System EV Integration," IEEE Trans. Smart Grid, vol. 9, no. 1, pp. 152-162, 2018.

[30] J. Y. Yong, V. K. Ramachandaramurthy, K. M. Tan and J. Selvaraj, "Experimental Validation of a Three- Phase Off-Board Electric Vehicle Charger With New Power Grid Voltage Control," IEEE Trans. Smart Grid, vol. 9, no. 4, pp. 2703-2713, July 2018.

[31] M. Nikkhah Mojdehi and P. Ghosh, "An On-Demand Compensation Function for an EV as a Reactive Power Service Provider," IEEE Trans. Vehicular Technology, vol. 65, no. 6, pp. 4572-4583, June 2016.

[32] U. R. Prasanna, A. K. Singh and K. Rajashekara, "Novel Bidirectional Single-phase Single-Stage Isolated AC–DC Converter With PFC for Charging of Electric Vehicles," IEEE Trans. Transportation Electrification, vol. 3, no. 3, pp. 536-544, Sept. 2017.

